World Journal of Engineering Research and Technology
WJERT
www.wjert.org
SJIF Impact Factor: 5.218

DEVICE SIMULATION AND SPECTRAL EFFICIENCY IMPROVEMENT OF SILICON BASED SOLAR CELL USING MULTI LAYER ANTI REFLECTING COATING

[1]*Aman Sharma and [2]Anil Boyal

[1]M.Tech.(Scholar) Department of Power System Engineering, Regional College For Education Research and Technology, Sitapura (Jaipur) (Rajasthan Technical University, Kota) India.

[2]Associate Professor, Department of Electrical Engineering Regional College for Education Research and Technology, Sitapura (Jaipur) (Rajasthan Technical University, Kota) India.

Article Received on 04/10/2018 **Article Revised on 25/10/2018** **Article Accepted on 15/11/2018**

***Corresponding Author**
Aman Sharma
M.Tech.(Scholar) Department of Power System Engineering, Regional College For Education Research and Technology, Sitapura (Jaipur) (Rajasthan Technical University, Kota) India.
DOI: 10.20959/wjert20184-1010

ABSTRACT

Efficiency improvement of solar cell has been achieved using design and simulation of anti-reflecting coating. Anti-Reflecting coating helps in deploying new geometries shape for the evaluation of different methods to provide for light trapping in all directions and enables full space utilization when bringing together into device arrays. Efficiency improvement strategies have been discussed using efficient selection of modules and surface texturing using TCAD tools. Significant improvement in yield and minimization of losses was achieved using device simulation and process simulation platform using silvaco tools. Multi-layer anti reflecting coating has been designed which can be studied to analyze the performance of system. It was observed that multi-layer coating helps in improvement of available current for similar light beam under simulation.

KEYWORDS: Anti Reflecting coating, TCAD, Device Simulation, Solar Cell.

I. INTRODUCTION

Now a day the world has depended on fossil fuels for energy supply. The worldwide consumption of fossil fuels (coal, gas and oil) is still increasing in spite of the growing global

awareness of the environmental impact of fossil fuel consumption and of limited fossil fuel reserves. Presently increase in the price of oil has been a most important source of economic problem in the world. The primary obstacle in the growth of photovoltaics is the high total cost of photovoltaic installations. To increase the solar cells efficiency, we have different solar cell texture technique that aims to maximize the incident photons absorption and the gathering of photo-generated carriers. Solar cell design in such a way that the specification of the parameters in order to maximize efficiency. Historically, higher efficiencies have been achieved by minimization of optical and electrical losses of silicon (si) solar cells.PV array is using an inverter which converts the DC power into AC power and output fed into the different load like motor, lighting loads and other loads. Modules are connected in series to get more of the rated voltage, and then in parallel to meet the current specification, as shown in Figure 1.1.

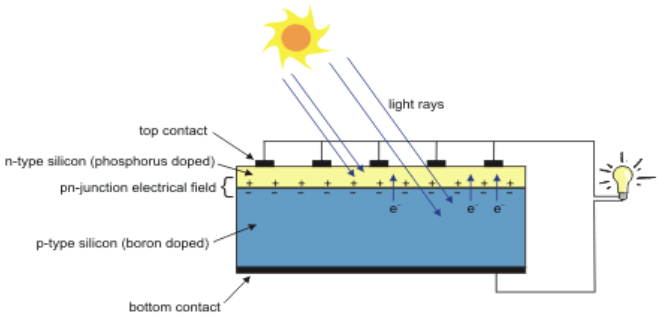

Fig. 1.1: Structure of a PV Cell.

Fig. 1.2: Different PV Modules.

Typically, a high transmittance and high electrical conductivity such as indium tin oxide film, a conductive polymer or a conductive nano-wire network are used for this purpose.

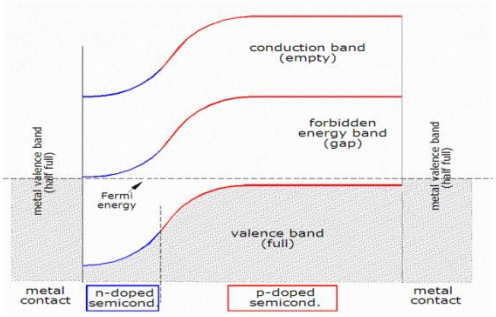

Fig. 1.3: Band diagram.

Silicon is a quadruple coordination atom, typically tetrahedral bonded to four adjacent silicon atoms. Tandem solar cells are attractive because they can be manufactured using a silicon single crystal with a band gap similar to, but easy to manufacture amorphous silicon.

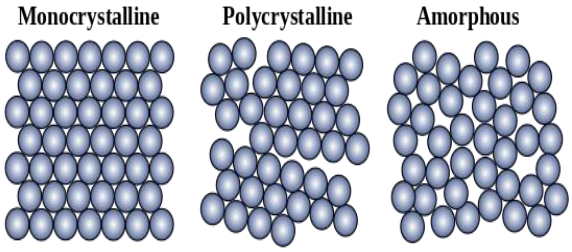

Fig. 1.4: Allotropic form of Silicon.

II. PHOTOVOLTIC EFFECT

The first Photovoltaic module was built by Bell laboraties in 1954.

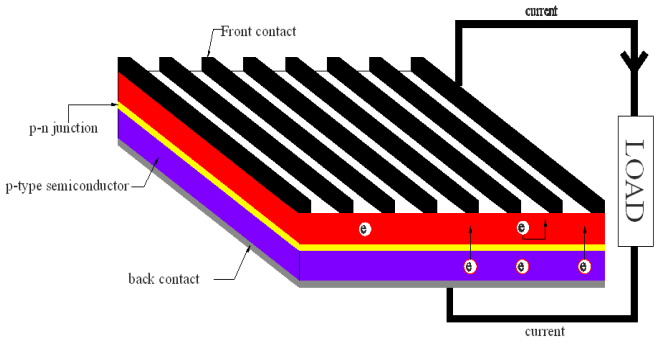

Figure 2.1: Basic diagram of Photoelectric effect.

Figure 2.1 shows the basic diagram of Photoelectric effect. In solar cell manufacture electric field is created by specially treating a thin semiconductor wafer. Modules are specially designed to produce voltage at a specific volt. However produced current will then depend upon the amount of light striking the module.

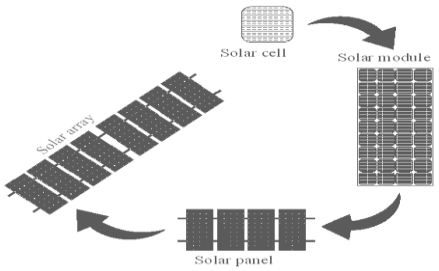

Figure 2.2: Representation of solar array.

$$I = I_L - I_D - I_{SH} \quad (2.1)$$

Where I is the total current generated by diode, I_L is photo generated current, I_D is the diode current and I_{SH} is the current through the shunt resistance.Voltage across these elements will give the value of current so

$$V_{jun} = V + IR_S \quad (2.2)$$

Where V_{jun} is the voltage across the diode and shunt resistance R_{SH}V=output terminal voltageI=output current R_S=series resistanceThe value of current through diode which is given by Shockley diode equation is-

$$I_D = I_0\left\{\exp\left[\frac{qV_{jun}}{nkT}\right]-1\right\} \quad (2.3)$$

Where I_0 =Reverse saturation currentn=diode Ideality factorq=elementary chargeK=Boltzmann's constantT=absolute TemperatureThe value of current through shunt resistance is given by

$$I_{sh} = \frac{V_{jun}}{R_{sh}} \quad (2.4)$$

Substituting the values in Equation (2.1), we get

$$I = I_L - I_o\left\{\exp\left[\frac{q(V+IR_S}{nKT}\right]-1\right\} - \frac{V+IR_S}{R_{SH}} \quad (2.5)$$

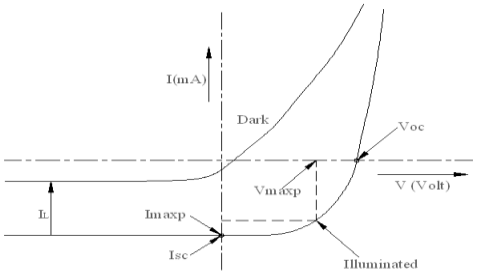

Figure 2.3: I-V characteristics of illuminated PV cell.

Figure 2.3 shows the I-V characteristics of illuminated PV cell. As the measuring voltage vary from 0 to Voc, the performance of various data are described as-

Open circuit voltage (Voc)It is the voltage appearing across the output terminal when the cell is operated in open circuit condition i.e. I=0.Neglecting the final term of characteristics equation due to high value of shunt resistance ,open circuit voltage is given as-

$$V_{oc} \approx \frac{nKT}{q} \ln\left(\frac{I_L}{I_0} + 1\right) \quad (2.6)$$

VOS is also defined as the maximum voltage difference across the cell for a forward-bias sweep in Power Quadrant.

Short circuit current (I_{sc})The current I which appears through the terminals under the condition of short circuiting the cell i.e. at v=0 is known as the short circuit current.

For a high quality solar cell having low value of Rs & I_0 and high value of Rsh

$I_{SC} \approx I_L$

I_{SC} is the maximum current value in power quadrant and occurs at the beginning of forward-bias sweep. Ideally this maximum current is the current which is produced by photo excitation.

Maximum power (P_{maxv}) From figure 2.4 it can be seen that at I_{SC} and V_{oc} the power deliver will be zero while the maximum condition will occur between these two conditions. The voltage and current at the condition of maximum power are V_{maxp}andI_{maxp}

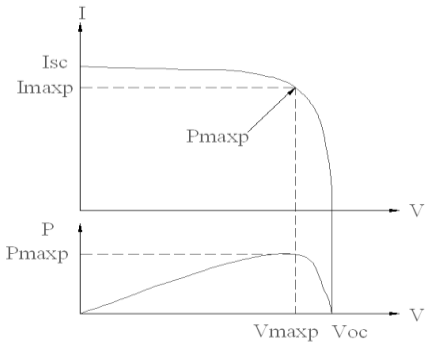

Figure 2.4: Power diagram.

The quality of solar cell is measured in terms of Fill factor (FF). It is a measure of sharpness of knee in the I-V curve. It is simply the ratio of maximum power to the theoretical power which is equal to the product of I_{sc}& V_{oc}.

High value of fill factor is desirable. Presence of series resistance will lower its value while its value will be high when open circuit voltage is high.

$$FF = \frac{P_{maxp}}{P_{Th}} = \frac{(I_{maxp} \times V_{maxp})}{I_{sc} \times V_{oc}} \qquad (2.7)$$

Typically fill factor ranges from 0.5 to 0.82

The efficiency of solar cell can be defined as ratio of electrical power output to the power input

$$\eta = \frac{P_{out}}{P_{in}}$$

The solar cell is operated upto its maximum efficiency and therefore

$$\eta_{max} = \frac{P_{max}}{P_{in}} \qquad \eta_{max} = \frac{P_{max}}{\text{Intensity of solar radiation X surface area of solar cell}}$$

$$\eta_{max} = \frac{V_{maxp} \times I_{maxp}}{I(t) \times Am} \qquad (2.8)$$

Where V_{maxp}, I_{maxp} are the voltage and current for maximum power corresponding to solar intensity I (t).

III. METHOLODOGY

Round cells are less expensive than semi-round or square cells since because material is lost in the production. They are rarely used because they do not use the module space. Figure 3.1 shows the monocrystalline solar cell.

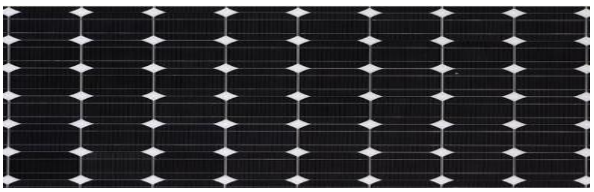

Fig. 3.1: Monocrystalline Solar Cell.

By using larger cells the module cost will be lower, because less number of cells is used. Figure 3.2 shows a polycrystalline cell.

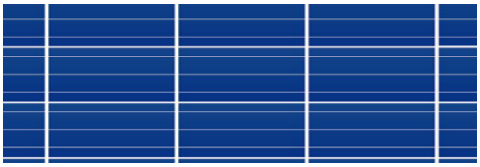

Fig. 3.2: Polycrystalline Solar Cell.

A solar cell made of a p-n junction is called a p-n solar cell. It is able to absorb photons and convert them into electricity.

The total p-n junction current I is

$I=I_L - I_F$ (3.1)

The block diagram of p-n junction solar cell is shown in Fig.3.3.

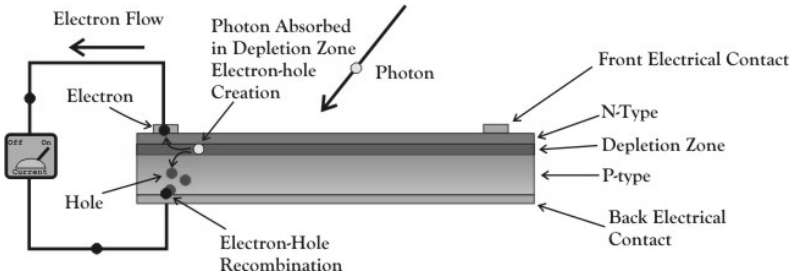

Fig. 3.3: PN Junction Solar Cell.

The efficiency of a solar cell is given by

$$\eta = \frac{FFV_{OC}Jsc}{P_{in}} \quad (3.2)$$

where Pin= incident powerFF = fill factor Jsc= short-circuit current density Voc=open circuit voltage.

The photons of incident light energy

$$E_{ph(\lambda)=\frac{hc}{\lambda}} \quad (3.3)$$

Where: Eph = photon energy of light (J), h = Planck's constant=$6.626*10^{-34}$ (Js). c = speed of light in a vacuum= $2.998*10^{8}$ (m/s). λ = wavelength (m).

The absorption coefficient is related to the extinction coefficient and the wavelength given by

$$\alpha(\lambda)=\frac{4\pi Ke}{\lambda} \quad (3.4)$$

Where: α = absorption coefficient (m^{-1}).ke = extinction coefficient.As the light propagates through the material the light intensity (I), at any point or depth in the material is given.

$I=I_o\, e^{-ax}$ (3.5)

Where: I_o = light intensity. x = path length of light.

Thus, when light is absorbed and generated electron hole pairs then $G_{e\text{-}h}$ generation rate at any depth of the material can be given by a differentiation equation.

$G_{eh=\alpha No}e^{-ax}$ (3.6)

Where: N_0= photon flux of the top surface (photons/unit-area/sec).The spectral characteristic SR (λ) in (A / W) of the solar cell is related to the external quantum efficiency by:

$SR(\lambda)=\frac{I_{SC}}{P_{in(\lambda)}}=\frac{qn_e}{\frac{hc}{\lambda}n_{ph}}=\frac{q\lambda}{hc}EQE(\lambda)$ (3.7)

Where: I_{SC} = short circuit current (A).$P_{in}(\lambda)$ = power of spectral incident light (W). q = electron elementary charge = $1.602*10^{-19}$ C.n_e = flux of electrons per unit time.

n_{ph} = incident flux of photons wavelength λ =per unit time. EQE = external quantum efficiency.The reflection as a function of the wavelength, R (λ), is given by:

$R(\lambda)=\frac{(n(\lambda)-1)^2}{(n(\lambda)+1)^2}$ (3.8)

Where n is the silicon refractive index and the medium from which light is transmitted is air with a refractive index equivalent to 1.

EQE=IQE(1-R-T) (3.9)

IQE = number of e-h pairs generated for photon of incident that are not reflected or transmitted through the cell.The standard way to find out the maximum output power Pmp of PV modules is given by:

$P_{mp=FFI_{SC}V_{oc}}$ (3.10)

Where: FF = fill factor of the.

V_{OC} = open circuit voltage.

The active area of the short circuit current per unit area or the density of the short-circuit current JSC (A / m2) can be expressed by

$J_{SC=}\int_{\lambda 2}^{\lambda 1}SR(\lambda)F(\lambda)T_g(\lambda)\left(1-R_g(\lambda)\right)T_{EVA}(\lambda)d\lambda$ (3.11)

$I_{SC}=J_{SC}A_{Cell}$ (3.12)

Where: $\lambda_{1\text{-}2}$ = spectral range of wavelengths (nm). F(λ) = spectral irradiance per unit area ($W/m^2/nm$). Tg(λ) = transmission of the covered glass, or portion of light not absorbed. Rg(λ) = reflectivity of the covered glass. $T_{EVA}(\lambda)$ = transmission of the encapsulated EVA.A_{cell}=

area of the solar cell (m^2).V_{OC} = maximum voltage, i.e. when no load is attached to the cell or zero current, and increases logarithmically with increasing daylight.

$$0 = I_{SC} - I_{D,0}\left(\frac{qv}{e^{KT_{CELL}n_{ideal}-1}}\right) \quad (3.13)$$

$$V_{OC} = \frac{KT_{CELL}}{q}\ln\left(\frac{I_{SC}}{I_{D,0}}+1\right) \quad (3.14)$$

Where: n_{ideal}= 214Ideality factor =1.K = Boltzmann's constant = 1.381*10^{-23} (m^2kg s^{-2}).T_{CELL} = absolute temperature (K).

$I_{D,0}$ = dark saturation current

Steps followed for Device Implementation:

Step 1: semiconductor material is used to design crystalline silicon solar cells.

Step 2: Mesh is defined in order to specify the x and y co-ordinates of device structure.

Step 3: Regions are define including region number and materials of the region.

Step 4: Electrodes are defined along its position and materials of the electrodes.

Step 5: Material properties are defined.

Step 6: Doping type (n or p- type) and doping concentration in each region is specified.

Step 7: Models are added for simulation process.

Step 8: Contact and interface provided and using SOLVE statement conditions for obtaining solution is defined.

Step 9: LOG File is created and saved the I-V characteristics of the device.

Step 10: Electrical and optical properties are simulated.

Step 11: Output is plotted in Tony plot and extracted for analysis.

IV. RESULTS AND DISCUSSIONS

A schematic of a fabrication layer for a silicon solar cell structure is shown in Figure 4.1 below:

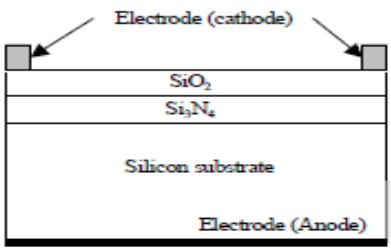

Fig. 4.1: Schematic Diagram of Proposed Structure.

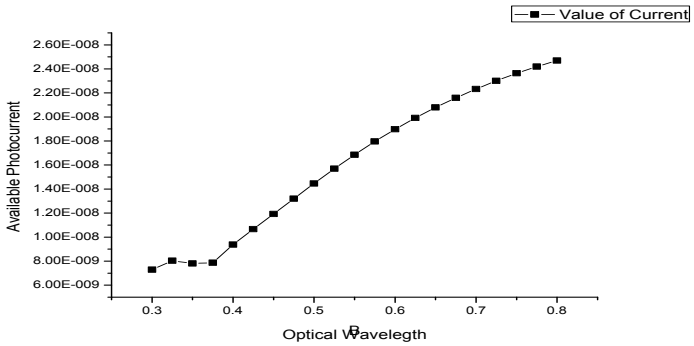

Fig.4.2: Photocurrent with respect to optical wavelength with two layer coating.

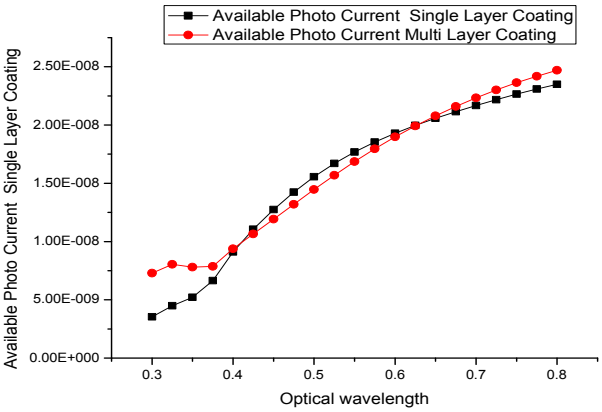

Fig. 4.3: Comparative Analysis of photocurrents with single layer and Multi-Layer coating.

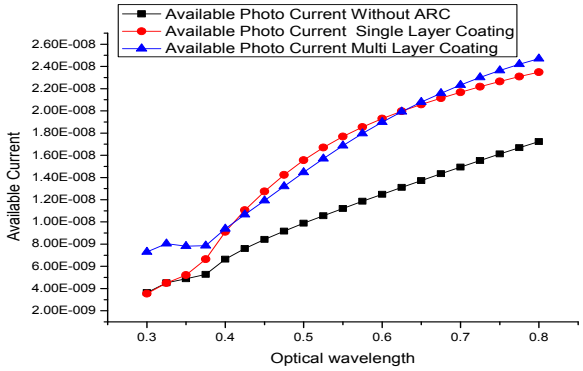

Fig. 4.4. Photocurrents without coating and with single layer and Multi-Layer coating.

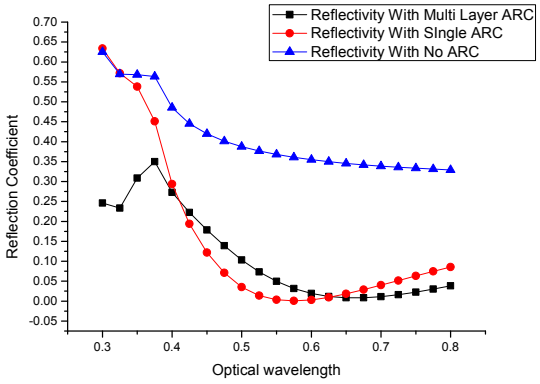

Fig. 4.5: Analysis of reflection coefficient with respect to anti reflecting coating.

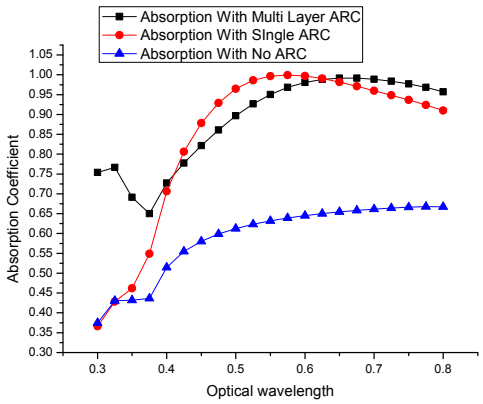

Fig. 4.6: Analysis of Absorption coefficient with respect to anti reflecting coating.

Figure 4.6 indicated the comparative analysis of absorption coefficients of all three proposed structure. The value of absorption coefficient of multi-layer coating is superior as compared to that of single layer coating and uncoated silicon cell in low wavelength and higher wavelength spectrum.

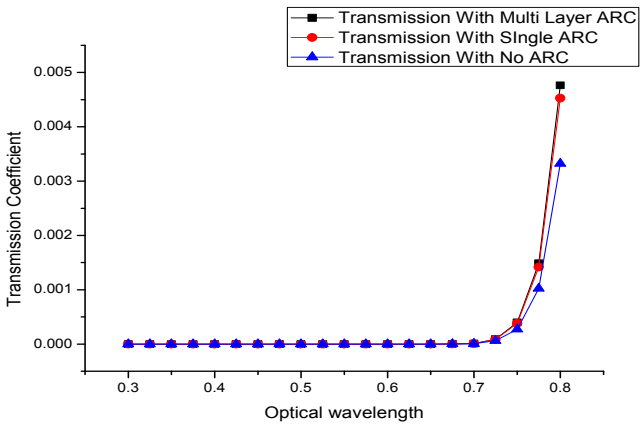

Fig.4.7: Analysis of transmission coefficient with respect to anti reflecting coating.

Figure 4.7 indicated the comparative analysis of transmission coefficients of all three proposed structure.

V. CONCLUSION

The proposed research was conducted on TCAD software using Silvaco Software package. 2D model of solar cell structure was developed. The structure of device was developed using Athena tool and process simulation was done using ATLAS toolbox. The performance of anti-reflecting coating was compared on parameters such as available photocurrent, absorption coefficients, reflection coefficients and transmission coefficients. Proposed two layer anti-reflecting coating shown better overall results with respect to light beam and it can be incorporated to enhance spectral efficiency of solar cell.Surface texturing with anti-reflecting coating of the photovoltaic cell, not only reduces the impact, but also contributes to the effect of a trapping of light, so that the advance of light is reflected by the inclined surfaces in a much wider range angles and thus increases the length of the path of light in the material absorbent. In fact, the internal reflection power in the silicon is higher because of the increase in light angles. The value of reflection coefficient of multi-layer coating is superior as compared to that of single layer coating and uncoated silicon cell.

VI. REFRENCES

1. G. Kumaravelu, M. M. Alkaisi and A. Bittar, "Surface texturing for silicon solar cells using reactive ion etching technique," Conference Record of the Twenty-Ninth IEEE Photovoltaic Specialists Conference, 2002; 2002: 258-261. doi: 10.1109/PVSC.2002.1190507.
2. Xiaorang Tian et al., "Pyramid size control and its effects on the performance of silicon heterojunction solar cells," 2015 China Semiconductor Technology International Conference, Shanghai, 2015; 1-3.doi: 10.1109/CSTIC.2015.715348.
3. Matthew B. Edwards Stuart," Texturing for heterojunction silicon solar cells", 1997 Energy Materials and Solar Cells, sumbitted for publication, doi:10.1.1.551.2790.
4. Macdonald, Daniel & Cuevas, Andres & Kerr, M.J. &Samundsett, C & Ruby, Douglas &Winderbaum, S & Leo, A. Texturing industrial multicrystalline silicon solar cells.Solar Energy, 2004; 76: 277-283. doi:10.1016/j.solener.2003.08.019.
5. M. Jalil, Saifuddin& Abdullah, Lennie& Ahmad, Ishak& Abdullah, Huda. The effect of surface texturing on GaAs solar cell using TCAD tools. IEEE International Conference

on Semiconductor Electronics, Proceedings, ICSE, 2008; 280283. doi:10.1109/SMELEC.2008.4770323.

6. Moreno, Mario &Daineka, D &Cabarrocas, Pere, Plasma texturing for silicon solar cells: From pyramids to inverted pyramids-like structures. Solar Energy Materials and Solar Cells. 2010; 94: 733-737.doi:10.1016/j.solmat.2009.12.015.
7. E. Manea et al., "Front Surface Texturing Processes for Silicon Solar Cells," International Semiconductor Conference, Sinaia, 2007; 191-194.doi: 10.1109/SMICND.2007.4519678.
8. Park, Hayoung& Kwon, Soonwoo& Sung Lee, Joon& Jin Lim, Hee& Yoon, Sewang& Kim, Donghwan. Improvement on surface texturing of single crystalline silicon for solar cells by saw-damage etching using an acidic solution.Solar Energy Materials and Solar Cells, 2009; 93: 1773-1778. 10.1016/j.solmat.2009.06.012.
9. Kim, Jeehwan& Inns, Daniel &Fogel, Keith &Sadana, Devendra. Surface texturing of single-crystalline silicon solar cells using low density SiO2 films as an anisotropic etch mask. Solar Energy Materials and Solar Cells, 2010; 94: 2091–2093. 10.1016/j.solmat.2010.06.026.
10. NiragKadakia and Sebastian Naczas and HassaramBakhru and Mengbing Huang" Fabrication of surface textures by ion implantation for antireflection of silicon crystals", Applied Physics Letters, 2010; 97(19): Pages.191912 doi:10.1063/1.3515842.
11. Cheng, Yuang-Tung & Ho, Jyh-Jier& Tsai, Song-Yeu& Ye, Zong-Zhi& Lee, William & Hwang, Daw-Shang & Chang, Shun-Hsyung& Chang, Chiu-Cheng & Wang, Kang. Efficiency improved by acid texturization for multi-crystalline silicon solar cells. Solar Energy, 2011; 85. 87-94. 10.1016/j.solener.2010.10.020.
12. A. Assi and M. Al-Amin, "Enhancement of electrical performance of acid textured multi crystalline silicon solar cells," International Conference on Renewable Energies, Y.28. Lee and D. Gong, Stability of SiNx/SiNx double stack antireflective coating for single crystalline silicon Solar cells, Nanoscale Research Letters, 2012; 50(7): 1-6. Doi: 10.1186/1556-276X-7-50.
13. K. Choi and K. J. Kim, Antireflection coating of a SiO/SiN double layer on silicon fabricated by magnetron sputtering, Journal Ceram Process, 2010; 11(3): 34130. M. Lipinski and al, Silicon nitride for photovoltaic application, Archives of Materials Science and Engineering, 2010; 6(2): 69-87. Reading direct: archivesmse.org/vol46_2/4621.
14. M. A. Green, M. Keevers, Optical properties of intrinsic silicon at 300 K, Journal Progress in Photovoltaic, 1995; 3(3): 189-192. Doi: 10.1002/pip.4670030303.

15. W. Lijuan, Z. Feng, Y. Ying, Z. Yan, L. Shaoqing, H. Shesong, N. Haiqiao and N. Zhichuan, Journal Semiconductor, 32(6), Doi:10.1088/1674-4926/32/6/066001.
16. M. Lipinski, P. Zieba, S. Jonas, S. Kluska, M. Sokolowski, and H. Czternastek, Optimization of SiNx: H layer for multicrystalline silicon solar cells, Optoelectronics Review, 2014; 12(1): 41-44. Doi:10.1109/MWC.2006.1593528.
17. M. C. Troparevski, A. S. Sabau, A. R. Lupini and Z. Zhang, Transfer-Matrix formalism for the calculation of optical response in multilayer systems : from coherent to incoherent interference, Optics Express, 2010; 18(24): 24745-24721. Doi: 10.1364/OE.18.024715.
18. P. Kosoboutskyy, M. Karkulovska and A. Morgulis, The principal of multilayer plane-parallel structure antireflection, Journal Optical Applied, 2010; 40(4): 759-765. Online: bvmeta1.element.baztech-article-BPW7-0014-0024.
19. C. C. Katsidis and D. I. Siapkas, General transfer-matrix method for optical multilayer systems with coherent, partially, coherent, and incoherent interference, Applied Optics, 2002; 41(19): 3978-3987. Doi: 10.1364/AO.41.003978.
20. L. Remache, A. Mahdjoud, E. Fourmond, J. Dupuis and M. Lemiti, Design of porous silicon,/PECVD SiOx antireflection coatings for silicon solar cells, Proceeding of international conference on renewable energies and power quality (ICREPQ), Granada, Spain, Mars, 23-25.
21. Y. Lee, D. Gong, N. Balaji and J. Yi, Stability of SiNx/SiNx double stack antireflection coating for single crystalline silicon solar cells, Nanoscale Research Letters, 2012; 7(50): 1-6. Doi: 10.1186/1556-276X-7-50.
22. A. Mahdjoub and al, Grated refraction index antireflection coatings based on silicon and titanium oxides, Semiconductor Physical Quantum Electronic and Optoelectronic, 2007; 60(1): 60-66. online: PALS 42.79.Wc,81/15.-z.
23. S. A. Boden, D. M. Bagnall, Sunrise to sunset optimization of thin film antireflective coatings for encapsulated, planar silicon solar cells, Progress Phovoltaic: Research Applied, 2009; 17(4): 241-252.Doi: 10.1002/pip.884.
24. D. Bouhafs, A. Moussi, A. Chikouche and J. M. Ruiz, Design and simulation of antireflection coating systems for optoelectronic devices :Application to silicon solar cells, Solar Energy Materials Solar Cells, 1998; 52(1-2): 79-93. Doi: 10.1016/S0927-0248(97)00273-0.
25. Bayrak, Zehra Ural, et al. "A low-cost power management system design for residential hydrogen & solar energy based power plants." International Journal of Hydrogen Energy, 2016; 41(29): 12569-12581.

26. Uzunoglu, M., and M. S. Alam."Dynamic modeling, design, and simulation of a combined PEM fuel cell and ultracapacitor system for stand-alone residential applications." IEEE Transactions on Energy Conversion, 2006; 21(3): 767-775.